Tuning the FMM-SABR for RFR caplets

Marcelo Taipe

July 25, 2022

Abstract

We review the extension to the Forward-Market-Model proposed by Willems (2020) to accommodate backward and forward-looking caplets within the same model. While theoretically intuitive, this extension offers very limited flexibility when calibrated to market data. We find that the backward and forward-looking smiles must share the same skew parameter. Moreover, the level and curvature parameters are only allowed to move in the same scale and direction by a bounded amount determined by the maturity. To address these limitations, we define new effective parameters by revisiting the SABR model with time dependent coefficients of Hagan et al. (2018). These new parameters allow the model to incorporate both kinds of caplets with less restrictions.

1 Introduction

After the significant upheaval and reform brought about by the Barclay's scandal in 2012, the financial world prepared for an impending transition away from IBOR rates. Its lack of transparency and the fact that rates were not based on actual transactions, among other factors, sealed the discontinuation of LIBOR as a reference rate for derivatives and other financial contracts. Following an announcement from British regulator in 2017, panel banks were compelled to sustain LIBOR until end-2021, by which time market participants were expected to agree on alternative reference rates. The consensus being that Risk-Free Rates (RFR) based on existing and liquid overnight markets would be chosen to replace LIBOR

(Bailey 2017).

This has proven to be the case as interest rate markets and fallback positions on derivatives contracts are increasingly favoring the use of these rates. Notorious examples are the embrace of SOFR in the US, SONIA in the UK, and SARON in Switzerland.

Although the RFRs overcome the transaction-based issue of the IBORs, they do not come without caveats. Their overnight nature makes them fundamentally different from LIBOR in the sense that they are not term rates. In order for them to act as underlyings, they have to be compounded daily over the duration of the reference period, which implies that contracts are set in-arrears. In fact, this compounding setting in arrears approach has been the ISDA proposal for replacing IBOR rates in derivatives contracts (Henrard 2019).

As liquidity and the introduction of new financial instruments is on the rise, there is a natural need for modeling RFRs rates and its related products. A good starting point are plain vanilla instruments, and more specifically caplets/foorlets. Although more of an essential unit for cap/floor pricing than actual traded contracts, caplets serve an important role in financial risk management. Managing large books of derivatives often involve constructing smiles where caplets are a staple component.

Several papers have already pointed out and explored the implications of the backward-looking nature of RFR for modeling purposes (Piterbarg 2020). One of those efforts is the Foward Market Model (FMM) introduced in the seminal work of Lyashenko and Mercurio (2019). The FMM allows for the modeling of RFR forward term rates while preserving its ability to model the classic forward rates based on IBORs. This is achieved through two ingenious definitions. One is the extended hybrid numeraire based on the bank account, and the other is the introduction of volatility decay function that reflects the fact that realized overnight rates decrease the uncertainty about the final compounded rate. Using a single model for both kind of rates is a handy feature as all the LMM tools for pricing forward looking instruments are also available for pricing backward looking ones. Nevertheless, as it is the case for the LMM, some important limitations linger in the FMM. Models with constant volatility are unable to reproduce the implied volatility smile, a conspicuous trait that characterizes option markets. One of the most adopted extensions to the LMM that enables it to reproduce this feature is the SABR model. In this setup, a set of four parameters is used to fit volatility smiles in a parsimonious manner. However, since the volatility decay function depends on time, adapting the SABR model to the FMM is not as straightforward as in the LMM. This task requires defining the SABR model with parameters that also depend on time. Such specification of the SABR model has been previously discussed in the literature to tackle similar problems (see Wang 2007, Chen et al. 2011, Van der Stoep et al. 2015, Hagan et al. 2018). In Willems (2020), the SABR model with time dependent coefficients of Hagan et al. (2018) is leveraged to come up with effective parameters that account for the volatility decay function. A new parameter that controls the speed of decay determines how the constant parameter differ from the effective parameters, which are the corresponding SABR parameters used for the backward smile. As a result, the FMM-SABR can reproduce volatility smiles for both backward and forward looking rates.

Because of its direct relationship with the LMM-SABR, the FMM-SABR proposed by Willems (2020) is quite intuitive and relatively simple to implement. However, the nature of the proposed effective parameters suggests that the backward smile is restricted to a particular shape once the forward smile is calibrated. We study this limitation and find that it doesn't conform to actual market data. The model offers poor smile fits when calibrated to options on Eurodollar and SOFR futures. In order to improve the model fit, we revisit the general version of the model presented in Hagan et al. (2018) and obtain new effective parameters that offer a better fit to the backward smile by allowing the alpha rho and nu parameters to be piece-wise constant. We test this new parameters and find that they allow the FMM-SABR to incorporate both backward and forward-looking smiles simultaneously.

The remainder of this work is structured as follows. Section 2 reviews the theoretical framework for pricing backward-looking caplets in the context of the FMM. Section 3 explores the limitations of the effective parameters introduced by Willems (2020) with respect to the parameter that controls the speed of volatility decay before calibrating the model to market data. Section 4 addresses the limitations by defining new effective parameters and testing their effectiveness. Section 5 concludes the article.

2 Theoretical Framework

The transition of IBORs towards overnight risk free rates comprises an adjustment of the modeling framework employed for caplets on term rates. Unlike IBORs, overnight rates have only one tenor (overnight) and are based on past transactions, which implies that the rate is known ex post. As a consequence, for RFRs to replace IBORs they have to act as term rates. There are two possible paths for this to be the case. The first is the daily compounding in-arrears of RFRs over the duration of the reference or accrual period, i.e., the length of the tenor. This proposal is in line with its ex post nature and means that the underlying rate is backward-looking. The second is constructing a measure of future projection for the final compounded rate based on market expectations implied from liquid instruments such as forwards or futures. This proposal is similar to the forward-looking nature of IBORs. Nevertheless, fallback positions seem to have favored the former, except in special cases where there is a special need for a forward-looking benchmark.

2.1 The FMM-SABR

When expectations of RFRs are used as term rates, the same modeling approach for IBORs caplets applies. Of more interest to this work is the case where RFRs are compounded in-arrears. For this case, we start by defining the modeling object as in Willems (2020). Let R be the approximate daily compounded in-arrears rate for the accrual period $[\tau_0, \tau_1]$:

$$R = \frac{1}{(\tau_1 - \tau_0)} \left(e^{\int_{\tau_0}^{\tau_1} r(u)} - 1 \right)$$

where $r(u)$ is the instantaneous RFR proxy. The proxy represents the fact that overnight rates are fixed daily rather than continuously.

Consider a filtered probability space $(\Omega, \mathcal{F}, (\mathcal{F}_t)_t, Q^{\tau_1})$ whose τ_1-forward measure Q^{τ_1} is associated with the hybrid numeraire defined in Lyashenko and Mercurio (2019). Under this measure, the backward-looking forward rate is $\mathcal{F}_{\tau_1}$ measurable and is defined as:

$$R(t) = E^{\tau_1}\left[R|\mathcal{F}_t\right].$$

where $R(t)$ is a martingale under Q^{τ_1}.

Now we can present the dynamics of the FMM-SABR for the special case of one tenor introduced in Willems (2020). Henceforth, in order to distinguish it from the standard SABR model, we will refer to this model simply as FMM-SABR.

$$dR(t) = A(t)\psi(t)R(t)^{\beta}dW_1(t), \quad \psi(t) = \min\left(1, \frac{\tau_1 - t}{\tau_1 - \tau_0}\right)^q \tag{1}$$

$$dA(t) = \nu A(t)dW_2(t), \quad A(0) = \alpha \tag{2}$$

$$dW_1(t)dW_2(t) = \rho dt, \tag{3}$$

The shift parameter s has been omitted since it does not affect the conclusions drawn from the model. Note that this is the standard SABR dynamics except for two distinctions related to the nature of backward-looking rates. First, in the standard SABR, $R(t)$ fixes at $t = \tau_0$ because term rates are forward looking. In contrast, RFRs are compounded in-arrears and thus fix at the end of the accrual period. This is possible due to the hybrid numeraire which allows the FMM-SABR to evolve stochastically up to $t = \tau_1$. Second, as time passes during the accrual period, daily fixings are realized which reduces the uncertainty about the final value of the compounded rate. This trait is reflected in the introduction of the volatility decay function $\psi(t)$. The new parameter $q > 0$ controls the speed of decay and allows for a concave or convex-like decay.

2.2 Pricing caplets under the FMM-SABR

We now define the payoffs for forward and backward-looking caplets with strike K and maturity at time $t = \tau_1$:

- forward looking: $(R(\tau_0) - K)^+$
- backward looking: $(R(\tau_1) - K)^+$

Note that the difference between these payoffs lays in that the forward one is known at $t = \tau_0$, that is, the beginning of the accrual period, while the backward one is known after all daily fixings have been realized at $t = \tau_1$. This results in an important and, by now, well known relationship between these payoffs. For $t \leq \tau_0$, using the Jensen inequality and the law of iterated expectations yields:

$$E^{\tau_1}\left[(R(\tau_0) - K)^+ \,|\mathcal{F}_t\right] \leq E^{\tau_1}\{E^{\tau_1}\left[(R(\tau_0) - K)^+ \,|\mathcal{F}_{\tau_0}\right] |\mathcal{F}_t\} \tag{4}$$

This implies that backward-looking caplets evolve stochastically after $t = \tau_0$ which, in turn, means that there is more volatility to be priced leading to backward-looking caplets being priced higher. This feature is naturally embedded into the FMM by means of the hybrid numeraire mentioned earlier.

Pricing forward-looking caplets reduces to using the standard SABR model since the rate evolves up until $t = \tau_0$ and $\psi(t) = 1$ for $t \leq \tau_0$. Therefore, the price at $t = 0$ of a forward-looking caplet is given by:

$$\begin{aligned} V^f(0) &= P(0,\tau_1) Black\left(R(0), K, \sigma^f_{IV}, \tau_0\right), \\ \sigma^f_{IV} &= \sigma_{hagan}(R(0), K, \alpha, \beta, \rho, \nu, \tau_0) \end{aligned} \tag{5}$$

where $Black$ is the formula from Black (1976) and σ_{hagan} is the lognormal approximation for the implied volatility derived in Hagan et al. (2002). Explicit expressions can be found in appendix A.

Pricing backward-looking caplets requires the model to evolve up until $t = \tau_1$. This means that there is a time dependence on the volatility parameter because $\psi(t) = \left(\frac{\tau_1 - t}{\tau_1 - \tau_0}\right)^q$ for $\tau_0 < t \leq \tau_1$. As a result, the Hagan approximation no longer holds. In order to circumvent this problem, Willems (2020) employs the results from the SABR model with time dependent parameters presented in Hagan et al. (2018), where effective parameters are introduced in order to use the original Hagan approximation. Willems derives effective parameters $\hat{\alpha}$, $\hat{\rho}$ and $\hat{\nu}$ such that the price at $t = 0$ of a backward-looking caplet is given by:

$$\begin{aligned} V^b(0) &= P(0, \tau_1) Black\left(R(0), K, \sigma^b_{IV}, \tau_1\right), \\ \sigma^b_{IV} &= \sigma_{hagan}(R(0), K, \hat{\alpha}, \beta, \hat{\rho}, \hat{\nu}, \tau_1) \end{aligned} \tag{6}$$

with $\hat{\alpha}, \hat{\rho}, \hat{\nu}$ as defined in appendix A. Notice that β remains the same for both kinds of caplets since the model from Hagan et al. (2018) requires the backbone function to be the same across expirations. Apart from this, the formula differs on the time until expiration for the options. Whereas forward-looking rates set at $t = \tau_0$, backward ones do so at $t = \tau_1$. Another notable distinction is that the formulas for the effective parameters differ when pricing the caplets during the accrual period: $\tau_0 < t \leq \tau_1$. This reflects the fact that the backward-looking caplet depends only on the dynamics during the accrual period. See the appendix for explicit expressions.

Using (4) and carrying out elementary manipulations in formulas (5) and (6) lead to the following relationship between their volatilities:

$$\begin{aligned} \sigma^b_{IV} \tau_1^{1/2} &> \sigma^f_{IV} \tau_0^{1/2} \\ \frac{\sigma^b_{IV}}{\sigma^f_{IV}} &> \left(\frac{\tau_0}{\tau_1}\right)^{1/2} \end{aligned} \tag{7}$$

We will find this inequality useful when comparing the volatilities found in market data.

3 Calibration of the effective parameters

In this section we discuss the calibration approaches originally proposed for the FMM-SABR. We study the behavior of the calibration and then evaluate the performance of the model using market data.

There are two calibration approaches proposed in Willems (2020):

1. Calibrate α, ρ, ν to forward-looking caplets and then mark q to match the ATM backward-looking caplet.

2. Calibrate $\hat{\alpha}, \hat{\rho}, \hat{\nu}$ directly to backward-looking caplets and then fix the value of q exogenously.

The decision to favor one approach over another is suggested to be based on the liquidity of the contracts. Notwithstanding, we regard them merely as potential ways to apply the model and, for this reason, we omit the liquidity factor from the discussion.

It is relevant to point out that the second approach yields two sets of parameters α, ρ, ν. One from calibrating to the forward-looking caplets and the other being implied (after fixing q) from the effective parameters calibrated to the backward-looking caplets. Consequently, it results in two separate models for each kind of caplet. This is somewhat dissenting to what the purpose of the FMM is. Consolidating risks is carried out more efficiently under a single model[1]In fact, the FMM was proposed as a way to incorporate both backward and forward-looking forward rates into a single model (Lyashenko and Mercurio 2019). Being the FMM-SABR an extension of this model, it is intuitive to aim for a model that reproduces both smiles. Accordingly, it makes more sense to favor the first approach, which entails using a single set of parameters α, ρ, ν for both kinds of caplets.

1. This argument is analogous to the very same problem of modeling the smile, where the goal is to use a single model to price options with different strikes.

3.1 Speed of decay and effective parameters

We restrict our study to the effective parameters for $t < \tau_0$. The reason being that, during the accrual period, the forward-looking rate is constant which means there is no IV quotes to calibrate to. As only backward-looking quotes are available, the second calibration approach is more suitable.

Under the first approach, once the original SABR parameters α, ρ, ν are calibrated, the effective ones are entirely dictated by the parameter that controls the speed of decay q. The extent and the way that q affects these parameters will directly determine the smile shape for the backward-looking caplets[2]. The limit cases of the effective parameters has been studied in Willems (2020). However, a more thorough understanding can be drawn from plotting the effective parameters as functions of q. Figure 1 shows this relationship by plotting the ratio of the effective parameter to its respective constant parameter. This makes it easier to see the magnitude of the effect of q and from there infer the behavior of the backward-looking smile.

First, it can be readily seen that $\hat{\rho}$ virtually remains unchanged for any value of q. This implies that the model contemplates the same skew for both the backward and forward-looking smile. There is no way to alter the skew once ρ is calibrated. Second, and more revealing, both $\hat{\alpha}$ and $\hat{\rho}$ seem change in the same magnitude when q changes. We numerically[3] confirm this as shown in figure 2. This means that, given α and ν, their effective counterparts will be reduced in the exact same proportion for a given q. Thus, the parameters driving the level and curvature of the backward-looking smile will always change in the same magnitude and in the same direction.

Lemma 1 *Let α, ρ, ν be a set of calibrated parameters. Numerically, $\forall\ q > 0$, the original effective parameters satisfy:*

2. For a comprehensive and detailed description of how the SABR parameters influence the smile shape see Rebonato et al. (2009) and Crispoldi et al. (2016)

3. The fact that this result holds numerically suggests that if exact formulas were used, instead of $\mathcal{O}(\epsilon^2)$ approximations, the derivatives would be the same.

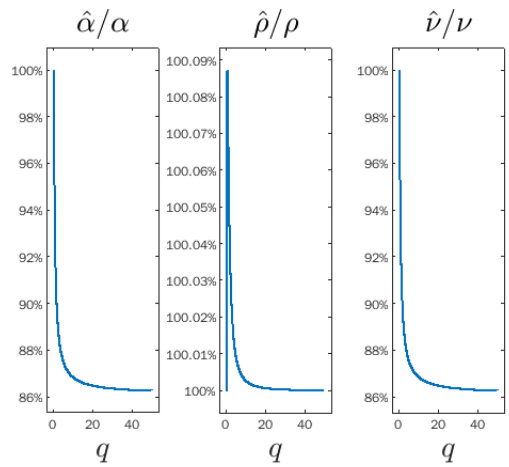

Figure 1: Dependence of effective parameters on q. Note that both $\hat{\alpha}$ and $\hat{\nu}$ are scaled by $(\tau_0/\tau_1)^{1/2}$ as $q \to \infty$. In this case, $\tau_0 = 0.75$ and $\tau_1 = 1$.

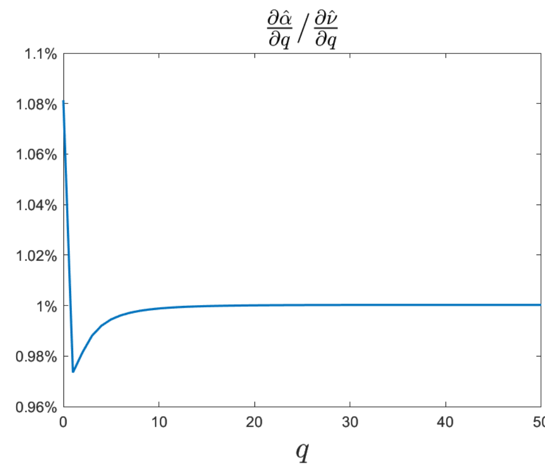

Figure 2: ratio of $\hat{\alpha}$ and $\hat{\nu}$ derivatives with respect to q

- $\hat{\alpha} = \alpha \times \delta < \alpha$
- $\hat{\rho} = \rho$
- $\hat{\nu} = \nu \times \delta < \nu$

where $(\tau_0/\tau_1)^{1/2} \leq \delta = \dfrac{\hat{\alpha}}{\alpha} = \dfrac{\hat{\nu}}{\nu} < 1$. *Evidently, these boundaries are defined by the limiting behavior of* q*:*

$$\lim_{q \to 0} \delta = 1 \qquad \lim_{q \to \infty} \delta = (\tau_0/\tau_1)^{1/2}$$

.

Again, this restricts the shape of the backward-looking smile but in a more contrived manner. The implications of these interactions are quite significant for a practical implementation of the model as is shown in the next subsection.

A direct application of lemma 1 allows for rewriting the price of the backward-looking caplet in terms of the forward-looking parameters, which gives rise to the following lemma:

Lemma 2 *For any* $\tau_0 < T < \tau_1$ *and setting* $\delta = (T/\tau_1)^{1/2}$, *equation* (6) *can be expressed as:*

$$Black\left(R(0), K, \sigma_{hagan}(R(0), K, \hat{\alpha}, \beta, \hat{\rho}, \hat{\nu}, \tau_1), \tau_1\right)$$

$$
\begin{aligned}
&= Black\left(R(0), K, \sigma_{hagan}(R(0), K, \left(\frac{\tau_1}{T}\right)^{1/2} \hat{\alpha}, \beta, \hat{\rho}, \left(\frac{\tau_1}{T}\right)^{1/2} \hat{\nu}, T), T\right) \\
&= Black\left(R(0), K, \sigma_{hagan}(R(0), K, \left(\frac{\tau_1}{T}\right)^{1/2} \alpha\delta, \beta, \hat{\rho}, \left(\frac{\tau_1}{T}\right)^{1/2} \nu\delta, T), T\right) \\
&= Black\left(R(0), K, \sigma_{hagan}(R(0), K, \alpha, \beta, \rho, \nu, T), T\right)
\end{aligned} \tag{8}
$$

This transformation allows us to shift the dependence on q to a single variable T. However, bear in mind that this transformation holds only when the effective parameters satisfy lemma 1.

It must be noted that the limiting behavior of T is defined implicitly in (8). By letting $q \to 0$, equation (6) reduces to equation 5 but with time-to-expiration $t = \tau_1$. Letting $q \to \infty$, equations (8) and (5) are equivalent. Then, we have that:

$$
\lim_{q \to \infty} T = \tau_0 \qquad \lim_{q \to 0} T = \tau_1 \tag{9}
$$

Isolating the dependence on q in a single variable T gives better insight about the functioning of the model. To see this, consider the following dynamics for $R(t)$:

$$
dR(t) = \sigma \min\left(1, \frac{\tau_1 - t}{\tau_1 - \tau_0}\right)^q R(t) dW(t)
$$

This is the constant volatility FMM for one tenor proposed in Lyashenko and Mercurio (2019) except for the inclusion of parameter q. Plus, if $t \leq \tau_0$, the dynamics reduces to the original Black's model. Therefore, pricing forward-looking caplets on $R(t)$ with fixing date $t = \tau_0$ yields the Black 76 formula. Relaxing the constant volatility assumption for a SABR-style volatility means that the correct price is given by equation (5). On the other hand, pricing backward-looking caplets on $R(t)$ with fixing date $t = \tau_1$ gives:

$$
Black\left(R(0), K, \sigma, \tau_0 + \frac{\tau_1 - \tau_0}{1 + 2q}\right)
$$

By comparing this formula with (8), it can be seen that the former is the constant volatility case of the latter. Then, a natural definition for T follows:

$$T = \tau_0 + \frac{\tau_1 - \tau_0}{1 + 2q} \tag{10}$$

This definition conforms with the limiting behavior of T implied by (8). Also, it gives a clear interpretation about the model: Pricing a backward-looking caplet is the same as pricing a forward-looking one. The only difference lies in the ”effective” time-to-expiration T used for the former, which, in turn, is completely determined by q. Succinctly, in the FMM-SABR the only difference between pricing backward and forward-looking caplets is time-to-maturity.

Lemma 2 can be applied to reduce the dimension of the calibration in q. That is, q can be directly implied without calibrating. To our understanding, there are two approaches to do this. First, q is implied given a set of calibrated parameters α, ρ, ν and an ATM quote for σ^b_{hagan}. A second route is implying q given two sets of separately calibrated parameters α, ρ, ν and $\hat{\alpha}, \hat{\rho}, \hat{\nu}$. In this case, if $\hat{\alpha}/\alpha \neq \hat{\nu}/\nu$, we will obtain two different values for q, which would suggest that the model is not well-specified. Bear in mind that both applications require T as given. Obtaining T in each method is relatively straightforward by applying lemma 1 and 2. However, since we are modifying the initial model, delving into these applications means drifting away from the objective of this work.

3.2 Calibrating the FMM-SABR to market data

While there is an ongoing transition towards RFRs, quotes for backward-looking caplets/caps are not readily available since they are mostly traded OTC. In order to have a more transparent and accessible source of data, we use implied volatility from options on Eurodollar and SOFR futures. Introduced in May 2018, 3-M and 1-M SOFR futures have experienced a significant increase in liquidity since they started trading (Skov and Skovmand 2021). Options on 3-M contracts have been available since early January 2020 with 1-M contracts

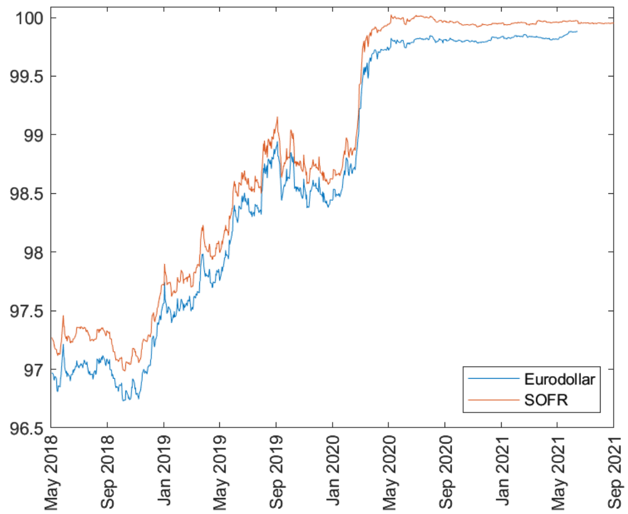

Figure 3: Prices for 3M futures contracts on Eurodollar and SOFR for June 2021

made available in May of the same year, following the success of the former as the transition unfolds (CME 2020). Given the greater liquidity of 3-M contracts, we use implied volatility data for this tenor. Using the SABR framework for pricing options on Eurodollar futures is not new in the literature (Wu 2012), (Zhang and Fabozzi 2016), (Feldman 2021). In fact, the original SABR article by Hagan et al. (2002) features this application of the model[4]. By using the FMM framework, we are able to account for the simultaneous modeling of the backward and forward-looking rates using a single stochastic factor. In practice, the evolution of the Eurodollar and SOFR futures appears to conform to this assumption. Figure 3 shows the historic price for Eurodollar and SOFR futures expiring in June 2021. Due to their backward-looking nature, SOFR contract does not fix until after the end of the accrual period, which in this case is the last day of August. Although the futures prices are not the same, it can be readily seen that both prices are driven by the same stochastic factor. Also, note that, as daily SOFR fixings are realized, volatility during the accrual period dwindles. A similar observation is pointed out in Lyashenko and Mercurio (2019) as a justification for the volatility decay function. Looking at different contract expirations, one can find the same pattern, which gives a sense of reassurance about using the model.

4. For a discussion of futures and the SABR model see West (2009).

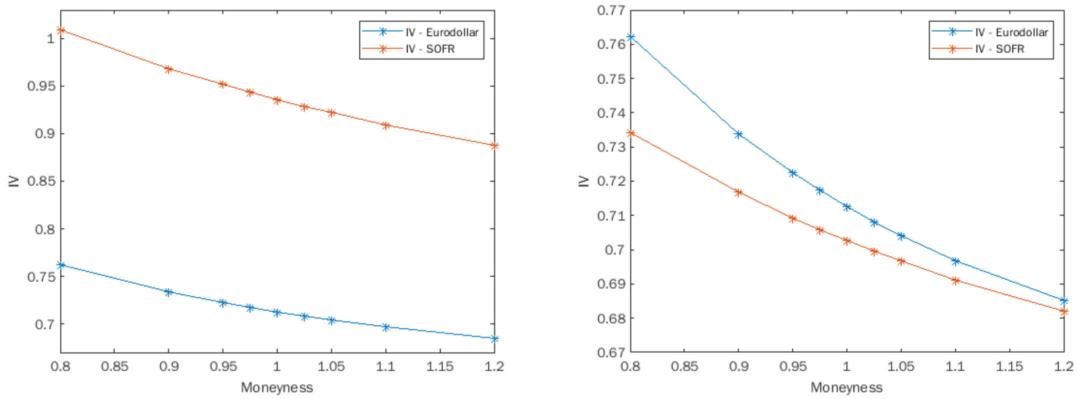

(a) Market IV (b) Adjusted IV

Figure 4: Market and adjusted IV from options on SOFR and Eurodollar 3M September 2022 futures. Data obtained on December 17, 2021.

Before tackling the calibration exercise, it is appropriate to discuss how the implied volatility (IV) is reported on markets. This is, indeed, a crucial step for the purpose of implementing the model. In Bloomberg terminals, the IV quotes from options on both Eurodollar and SOFR futures is obtained with respect to time-to-exercise τ_0. This is due to the fact that SOFR futures options stop trading at the start of the accrual period, i.e., when $t = \tau_0$; despite the underlying rate being active through $t = \tau_1$. This additional uncertainty is reflected by IV quotes for options on SOFR futures being higher than those for options on Eurodollar futures as can be seen in panel 4a for options expiring in September 2022. Consider equation (6), the FMM-SABR requires that IV for options on backward-looking rates be obtained with respect to time-to-exercise τ_1. Conforming to this technicality is straightforward. Notwithstanding, as suggested earlier, while the underlying rates share the same stochastic factor, they differ in price. This renders the volatility implied from the backward and forward-looking options not comparable. To overcome this problem, when implying the volatility from the price of the backward-looking option, instead of using the backward-looking rate, we use the value of the forward-looking rate as the spot rate[5]. In order to leave the level of moneyness unaltered, the strike price has to be adjusted accordingly. That is,

5. This can be done in the opposite way as well, by using the backward-looking spot rate when implying the volatility from the price of the forward-looking option

adding the difference between the backward and forward-looking spot rates to the strike. To sum up the procedure, the backward-looking implied volatility for options on SOFR futures is given by the value of $\tilde{\sigma}^b_{IV}$ that solves:

$$C_{market} = Black\left(100 - R(0), 100 - K + \tilde{R}(0) - R(0), \tilde{\sigma}^b_{IV}, \tau_1\right)$$

where C_{market} denotes the market price of the call option, $R(0)$ the spot price of the Eurodollar futures, $\tilde{R}(0)$ the spot price of the SOFR futures, and τ_1 the fixing date for SOFR futures. It is important to note that, since futures prices are quoted with the IMM convention, the Black put formula should be used to obtain the IV for calls, and vice versa. Panel 4b shows the same unaltered IV for Eurodollar options and the IV for SOFR options using this adjustment. The fact that the smile for SOFR options is now below the one of Eurodollars is contemplated by (7).

We are interested in pricing both backward and forward-looking options under the same model. Therefore, we use the first approach and calibrate the FMM-SABR to the IV for the March 2023, June 2023, September 2023, and December 2023 contracts for both SOFR and Eurodollar options with data obtained on December 17, 2021. First, we calibrate the original parameters α, ρ, ν to the IV of Eurodollar options for $\beta = 0.25, 5, 75$ and 1:

$$\min_{\rho,\nu} \quad \sum_{k\in K} \left[\sigma_{hagan}(R(0), k, \alpha(\rho, \nu, \sigma^{b-ATM}_{IV-Market}), \beta, \rho, \nu, \tau_1) - \sigma^{f}_{IV-Market}(k)\right]^2 \tag{11}$$

where $\alpha(\rho, \nu, \sigma^{f-ATM}_{IV-Market})$ indicates that West (2005)'s calibration method is being used. This involves a least-squares fitting problem where we use the Levenberg-Marquardt algorithm. The first row of figure 5 shows the fitted smiles for the Eurodollar contracts. As it is expected of the SABR model, the fit quality is excellent and does not depend on the value of β. Second, we calibrate q to SOFR market quotes using:

$$\min_{q} \sum_{k \in K} \left[\sigma_{hagan}(R(0), k, \hat{\alpha}(q), \beta, \hat{\rho}(q), \hat{\nu}(q), \tau_1) - \sigma^{b}_{IV-Market}(k)\right]^2 \tag{12}$$

In accordance with lemma 1, the calibrated parameters satisfy that $\hat{\alpha}/\alpha = \hat{\nu}/\nu$ and $\hat{\rho} \approx \rho$ for all contracts. In a somewhat counterintuitive manner, rather than signaling a good quality of calibration, this occurrence reveals a limitation of the model. The second row of figure 5 shows the fitted smiles for the SOFR contracts. The FMM-SABR offers a poor fit to these options across every expiration and every value of β. Also a common trait is that SOFR options exhibit a steeper or milder slope than the corresponding Eurodollar option, suggesting a different value for the slope parameter: $\hat{\rho} \neq \rho$. In terms of the alpha and nu parameters, it can not be assessed by direct observation whether the magnitude of change δ is appropriate to fit the smile or even if the magnitude is the same for both parameters. An inherent question rises, What are the values of the effective parameters that best fit the SOFR smiles? This point is addressed by carrying out a third calibration where the effective parameters are directly fitted to the SOFR IV:

$$\min_{\hat{\rho}, \hat{\nu}} \sum_{k \in K} \left[\sigma_{hagan}(R(0), k, \hat{\alpha}(\hat{\rho}, \hat{\nu}, \sigma^{b-ATM}_{IV-Market}), \beta, \hat{\rho}, \hat{\nu}, \tau_1) - \sigma^{b}_{IV-Market}(k)\right]^2 \tag{13}$$

The resulting fit is shown in the third row of figure 5. The quality of this calibration is essentially the same as the one carried out for the forward-looking options. As a result, the fitted smiles are up to par with the forward-looking ones.

Given that the same model is calibrated to the same data under different methods, the results of the one that offers the best fit can be treated as being ”correct”. Once the ”correct” values of the effective parameters are known, they can be compared with the ones obtained from calibrating q. Table 1 shows the ratio of the calibrated effective and original parameters for $\beta = 1$. As already pointed out, when q is calibrated, the ratios automatically conform to lemma 1. In contrast, when the effective parameters are calibrated directly, the ratios for

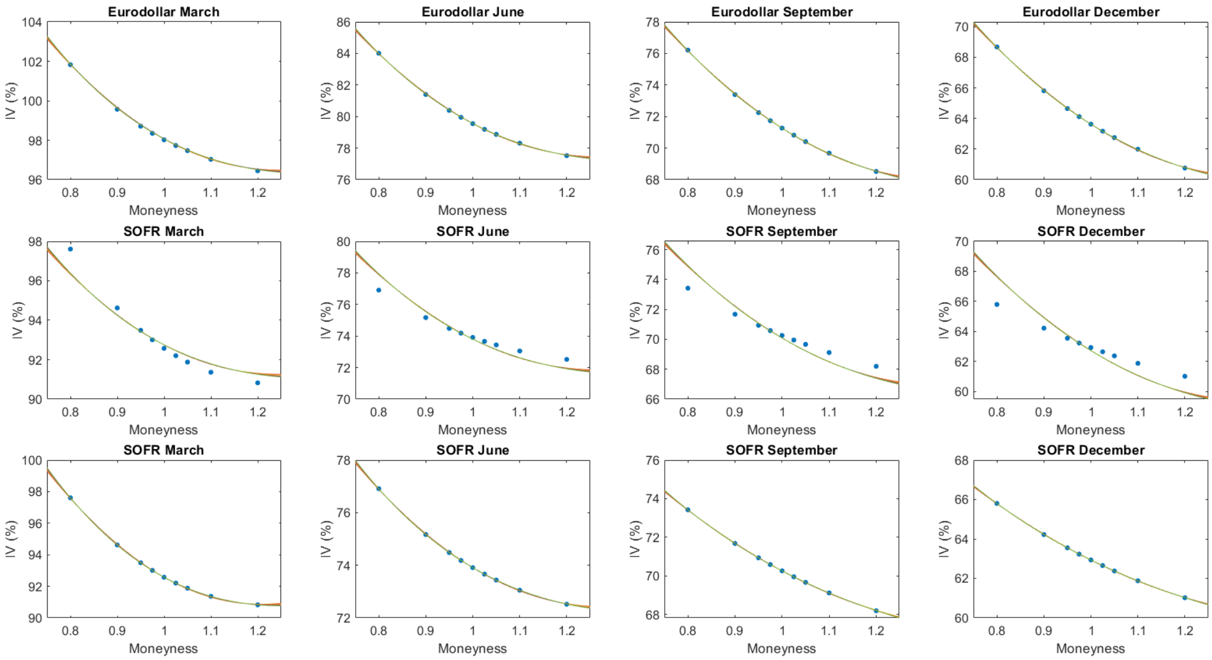

Figure 5: FMM-SABR smiles for $\beta = 0.25, 5, 75$ and 1. Contracts: March 23, June 23, September 23, and December 23 Eurodollar and SOFR options. Data obtained on December 17, 2021.

the alpha and nu parameters are not the same. Moreover, the values of the effective and original rho parameter are not equal. This pattern repeats for every expiration and reveals an important limitation from the model. If we were to ask for what is the "correct" value of q that is implied by directly calibrating the effective parameters, then we would find out that by having $\hat{\alpha}/\alpha \neq \hat{\nu}/\nu$, each effective parameter requires a different value for q. In fact, when these ratios are less than $(\tau_1/\tau_0)^{1/2}$, there is no value of q that matches the effective with the original parameter. Similarly, there is no value of q such that $\hat{\rho} \neq \rho$. An immediate conclusion is that the FMM-SABR is unable to fit both the backward and forward-looking smile if, after calibrating the effective and original parameters to the backward and forward-looking smiles, respectively, the ratio of effective to original parameters do not comply with lemma 1.

Expiration	$\left(\frac{\tau_0}{\tau_1}\right)^{1/2}$	Calibration method	$\frac{\hat{\alpha}}{\alpha}$	$\frac{\hat{\rho}}{\rho}$	$\frac{\hat{\nu}}{\nu}$
March 2023	68.5%	q	92%	100%	92%
		$\hat{\alpha}, \hat{\rho}, \hat{\nu}$	89%	104%	115%
June 2023	79.5%	q	91%	100%	91%
		$\hat{\alpha}, \hat{\rho}, \hat{\nu}$	93%	88%	77%
September 2023	86.1%	q	96%	100%	96%
		$\hat{\alpha}, \hat{\rho}, \hat{\nu}$	100%	106%	65%
December 2023	89.7%	q	97%	100%	97%
		$\hat{\alpha}, \hat{\rho}, \hat{\nu}$	102%	104%	60%

Table 1: Ratio of effective parameters to its standard values considering two calibration approaches for all expirations and $\beta = 1$. Time to expiration calculated using ACT/ACT convention. All values are expressed in percentage terms.

4 The SABR model with time-dependent parameters

This section addresses the limitations of the FMM-SABR raised in the previous section. But before proposing a solution, we think it is fundamental to first revisit and discuss the calibration procedure as it is where the limitation stems from, thereby giving us insight about how to approach a solution.

If the goal is to use a single model to reproduce both backward and forward-looking smiles, the initial proposal is to first calibrate the model to the forward-looking smile and then make q hit the backward-looking smile. However, we consider that there are two issues with this approach. First, trying to make q hit the backward-looking smile goes against the spirit of the SABR model. The appeal of the SABR framework is offering an effective way to fit smiles by having a closed-form expression for the volatility that depends on a set of parameters dictating its shape. Each parameters allows the model to capture one characteristic of the smile: level, skew and curvature. By calibrating q and not the parameters in the volatility formula, the model is not being used how it was intended and, more importantly, loses its full potential to fit smiles. Second, as seen in the previous section, this calibration procedure offers poor fits to market data and therefore is not reliable to be used in practice.

Based on the results of the previous section, both issues can be solved right away if the effective and original parameters are calibrated directly to its respective smiles. This is a more natural approach from a practical perspective but, at the same time, can be troublesome under the current framework. Since the goal is to use a single model for both types of options, the calibrated values of the effective and original parameters should be reconciled using a dependence established by the model. That is, there must be a solution for the system:

$$\begin{aligned} \hat{\alpha}(*) - \hat{\alpha}_c &= 0 \\ \hat{\rho}(*) - \hat{\rho}_c &= 0 \\ \hat{\nu}(*) - \hat{\nu}_c &= 0 \end{aligned} \tag{14}$$

where $(*)$ indicates the functional dependence of the effective parameters on other variables and the subscript c means the calibrated value of the parameter is being used. In the FMM-SABR, this dependence is based entirely on q. We have already seen that relying on q for this purpose is a very restricting choice. A solution for this reconciliation problem is guaranteed to exist only if the calibrated values of the parameters conform to lemma 1. In any other case, no solution exists and we are left with using separate models for each smile. The problem is now clear. We need to define a new dependence for the effective parameters such that they can be reconciled with the original ones regardless of whether they conform to lemma 1 or not.

4.1 Defining new effective parameters

Originally intended to fit volatility surfaces, the SABR model with time-dependent parameters presented in Hagan et al. (2018) was used by Willems (2020) to account for the time dependence in the volatility decay function of equation (1). The model itself is more general and discussing its proposed use can shed light about how to tackle the problem we are facing. In Hagan et al. (2018), the authors argue that, although the SABR model offers good fits to smiles for a given expiry T_i, different expiries require different values for the model parameters and, in turn, different models for each expiry. To make the SABR model able to accommodate all expiries, the parameters are allowed to depend on time and the following dynamics are proposed:

$$dR(t) = \sigma(t)\tilde{A}(t)R(t)^{\beta}dW_1(t) \tag{15}$$

$$d\tilde{A}(t) = \nu(t)\tilde{A}(t)dW_2(t), \quad \tilde{A}(0) = 1 \tag{16}$$

$$dW_1(t)dW_2(t) = \rho(t)dt, \tag{17}$$

Under this model, for a given expiry T_i, the IV approximation of Hagan et al. (2002) can be used to price European options on $R(t)$ by defining effective parameters as follows:

$$\hat{\alpha} = \Delta e^{\frac{1}{4}\Delta^2 G T_i}, \quad \hat{\rho} = \bar{b}/\sqrt{\bar{c}}, \quad \hat{\nu} = \Delta\sqrt{\bar{c}}, \tag{18}$$

where:

$$\begin{aligned}
\Delta^2 &= \frac{\tau\left(T_i\right)}{T_i} = \frac{1}{T_i}\int_0^{T_i} \sigma^2\left(s\right)ds, \\
\bar{b} &= \frac{2}{\tau\left(T_i\right)^2}\int_0^{T_i}\left[\tau\left(T_i\right) - \tau(s)\right]\rho(s)\nu(s)\sigma(s)ds, \\
\bar{c} &= \frac{3}{\tau\left(T_i\right)^3}\int_0^{T_i}\left[\tau\left(T_i\right) - \tau(s)\right]^2\nu^2(s)ds + \frac{9}{\tau\left(T_i\right)^3}\int_0^{T_i} I^2(s)\sigma^2(s)ds - 3\bar{b}^2, \\
G &= \frac{2}{\tau\left(T_i\right)^2}\int_0^{\tau_i}\left[\tau\left(T_i\right) - \tau(s)\right]\nu^2(s)ds - \bar{c}
\end{aligned}$$

with:

$$I(u) = \int_0^u \rho\left(s\right)\nu\left(s\right)\sigma\left(s\right)ds, \quad \tau\left(u\right) = \int_0^u \sigma^2(s)ds$$

In order to calibrate the model to the volatility surface, the effective parameters $\hat{\alpha}_i, \hat{\rho}_i, \hat{\nu}_i$ are calibrated directly to the smile of each expiry T_i. Then, the parameters in the functions defined for $\sigma(t)$, $\rho(t)$ and $\nu(t)$ are chosen such that they match the calibrated effective parameters. It is proposed that the simplest way to achieve this is by defining piece-wise constant parameters:

$$\sigma(t) = \sigma_i, \quad \rho(t) = \rho_i, \quad \nu(t) = \nu_i \quad \text{for} \quad T_{i-1} < T < T_i \tag{19}$$

The iterative process of matching the effective parameters starts with the earliest expiry, for which $\hat{\alpha}_0 = \alpha_0$, $\hat{\rho}_0 = \rho_0$, $\hat{\nu}_0 = \nu_0$, and ends at the longest expiry. This procedure is equivalent to solving system (14), except that, in that case, we are primarily relying on q to match the effective parameters.

In the context of the FMM-SABR, there are only two expiries (τ_0 and τ_1), and the parameters are kept constant across them. The only dependence of time is bore by the inclusion of the volatility decay function. Thus, the parameter functions are:

$$\sigma(t) = \alpha\psi(t), \quad \rho(t) = \rho, \quad \nu(t) = \nu \quad \text{for} \quad 0 < t < \tau_1 \tag{20}$$

Under this definition, the solutions of (18) for backward-looking options are equal to the ones proposed in Willems (2020). A logical way to give flexibility to the effective parameters, without unnecessarily adding complexity, is by also using a pice-wise approach.

Lemma 3 *Consider a set of expiries* $\{\tau_0, \tau_1\}$ *for equations* (15)-(17). *Define the functions for the time-dependent parameters:*

$$\sigma(t) = \begin{cases} \alpha_0\psi(t), & 0 < t < \tau_0 \\ \alpha_1\psi(t), & 0 < t < \tau_1 \end{cases}, \quad \rho(t) = \begin{cases} \rho_0, & 0 < t < \tau_0 \\ \rho_1, & 0 < t < \tau_1 \end{cases}, \quad \nu(t) = \begin{cases} \nu_0, & 0 < t < \tau_0 \\ \nu_1, & 0 < t < \tau_1 \end{cases}$$

By solving (18)*, the new effective parameters that go into formula* (6) *are:*

$$\hat{\alpha} = \begin{cases} \Delta_0 e^{\frac{1}{4}\Delta_0^2 G_0 \tau_1}, & 0 < t < \tau_0 \\ \Delta_1 e^{\frac{1}{4}\Delta_1^2 G_1 \tau_1}, & \tau_0 < t < \tau_1 \end{cases}, \quad \hat{\rho} = \begin{cases} \dfrac{\bar{b}_0}{\sqrt{\bar{c}_0}}, & 0 < t < \tau_0 \\ \dfrac{\bar{b}_1}{\sqrt{\bar{c}_1}}, & \tau_0 < t < \tau_1 \end{cases}, \quad \hat{\nu} = \begin{cases} \Delta_0 \bar{c}_0^{1/2}, & 0 < t < \tau_0 \\ \Delta_1 \bar{c}_1^{1/2}, & \tau_0 < t < \tau_1 \end{cases}$$

with $\Delta_0, \bar{b}_0, \bar{c}_0, G_0$ *and* $\Delta_1, \bar{b}_1, \bar{c}_1, G_1$ *as defined in appendixB .*

It is important to point out that all three effective parameters in this lemma depend on $\alpha_1, \rho_1, \nu_1, q$ for $0 < t < \tau_1$. In contrast, the dependence on α_0, ρ_0, ν_0 is only present during $0 < t < \tau_0$.

4.2 Testing the new effective parameters

Now that a new dependence for the effective parameters has been defined, our goal is to apply it to reconcile the calibration results presented previously. More specifically, we want to solve system (14), whose dependence is now given by:

$$\begin{aligned} \hat{\alpha}(\alpha_1, \rho_1, \nu_1, q) - \hat{\alpha}_c = 0 \\ \hat{\rho}(\alpha_1, \rho_1, \nu_1, q) - \hat{\rho}_c = 0 \\ \hat{\nu}(\alpha_1, \rho_1, \nu_1, q) - \hat{\nu}_c = 0 \end{aligned} \tag{21}$$

Note that there is no dependence on α_0, ρ_0, ν_0 because these are equivalent to the original parameters α, ρ, ν and thus their values are known after calibrating to the forward-looking smile. Consequently, we are left with an underdetermined non-linear system of equations. Nevertheless, the system is, in fact, determined. This is due to the nature of the procedure we are performing. In theory, given the calibrated values for the effective parameters, it is possible to obtain implicitly one of the unknown parameters.

We can attempt to reduce one of the unknowns by implying q from a previously defined function that depends on it, similar to how lemma (2) was applied to define (10) in terms of

q. Nevertheless, such procedure is only possible when lemma (1) holds. Since we are trying to escape the limitations of this lemma, we can not resort to this path.

Another path towards reducing the dimension of the unknowns is to imply one of the parameters $\alpha_1, \rho_1, \nu_1, q$ by inverting one of the formulas in lemma (3). This is similar to how α is implied using the method described in West (2005). The distinction lies in that we use the formulas of the effective parameters instead of the Hagan et al. (2002) approximation. The decision of which parameter to imply is determined by the complexity of the effective parameter formula. However, trying to solve these formulas for one of the parameters $\alpha_1, \rho_1, \nu_1, q$ is not plausible. A more reasonable approach is to use the inner components of these formulas. Specifically, by multiplying the effective parameters we can isolate some of these components and obtain more tractable expressions[6]:

$$\hat{\rho}_c \hat{\nu}_c = \bar{b}_0 \Delta_0$$

This equation can not be solved explicitly for q or α_1. Solving for ρ_1 or ν_1 is possible and both lead to similar solutions. Solving for ρ_1 yields:

$$\rho_1 = \frac{\hat{\rho}_c \hat{\nu}_c \theta^2 + \sqrt{\frac{\theta}{\tau_1}}\left[\nu_0\, \rho_0 \tau_0 ({\alpha_0}^3 \tau_0 - 2\alpha_1 \theta)\right]}{\frac{2\alpha_1^3 \nu_1 (\tau_0 - \tau_1)^2}{(3q+2)(2q+1)} \sqrt{\frac{\theta}{\tau_1}}} \tag{22}$$

where:

$$\theta = \alpha_0^2 \tau_0 + \frac{\alpha_1^2 (\tau_1 - \tau_0)}{2q+1}$$

In order to ensure we get a value for the correlation within $[-1, 1]$, we can express equation (22) as follows:

$$\tilde{\rho}_1 = sgn(\rho_1) \min\{|\rho_1|, 1\}$$

6. Although it may seem arbitrary, this is the most feasible way to get reduced expressions. The expressions of $\bar{c}$ and G are considerably larger and harder to solve for one of the parameters.

Expiration	$\boldsymbol{\beta = 0.25}$	$\boldsymbol{\beta = 0.5}$	$\boldsymbol{\beta = 0.75}$	$\boldsymbol{\beta = 1}$
March 2023	0.0348	0	0	0
June 2023	0	0	0	0
September 2023	0	0	0	0
December 2023	0	0	0	0

Table 2: RMSE for the solutions of system (21). Numbers rounded to the sixth decimal place.

Then, system (21) can be expressed as:

$$\begin{aligned} \hat{\alpha}(\alpha_1, \tilde{\rho}_1(\alpha_1, \nu_1, q), \nu_1, q) - \hat{\alpha}_c = 0 \\ \hat{\rho}(\alpha_1, \tilde{\rho}_1(\alpha_1, \nu_1, q), \nu_1, q) - \hat{\rho}_c = 0 \\ \hat{\nu}(\alpha_1, \tilde{\rho}_1(\alpha_1, \nu_1, q), \nu_1, q) - \hat{\nu}_c = 0 \end{aligned} \tag{23}$$

as before, we omit writing the dependence on α_0, ρ_0, ν_0 explicitly. The resulting system has as many unknowns as equations and can be solved using conventional numerical methods. Despite being quite straightforward to implement, one can opt for skipping this step by solving numerically the uderdetermined system (21) using an algorithm based on the Gauss-Newton method, e.g., the Levenberg-Marquardt algorithm. Nevertheless, having a determined system allows for more variety in the choose of the algorithm.

Tables 2 and 3 show the RMSE for the solutions of systems (21) and (23), respectively, using the calibrated values of $\hat{\alpha}_c, \hat{\rho}_c, \hat{\nu}_c$ obtained in the previous section. The results show that the new dependence of the effective parameters offers a perfect match across all expirations and is independent of the value of β. The only relative mismatch occurs in table 3 for the March parameters when $\beta = 0.25$, which is most likely due to the fact that we used the same starting values for the algorithm in all cases[7].

In order to better asses the performance of these new parameters, we repeat the exercise for shorter maturities[8] using option futures data for SOFR and Eurdollar contracts expiring

7. This is akin to how the calibration of the SABR parameters is highly influenced by the starting values used in the algorithm, which is another topic of study in itself with a good amount of literature covering it (Gauthier and Rivaille 2009), (Floc'h, Kennedy, et al. 2014).

8. We avoid testing the model in a longer maturity setup for two reasons. First, the open interest for

Expiration	$\beta = 0.25$	$\beta = 0.5$	$\beta = 0.75$	$\beta = 1$
March 2023	0	0	0	0
June 2023	0	0	0	0
September 2023	0	0	0	0
December 2023	0	0	0	0

Table 3: RMSE for the solutions of system (23). Numbers rounded to the sixth decimal place.

Expiration	$\beta = 0.25$	$\beta = 0.5$	$\beta = 0.75$	$\beta = 1$
March 2022	0	0	0	0
June 2022	0	0	0	0
September 2022	0	0	0	0
December 2022	0	0	0	0

Table 4: RMSE for the solutions of system (21). Numbers rounded to the sixth decimal place.

March 2022, June 2022, September 2022, and December 2022 obtained on December 17, 2021.

The RMSE reported in tables 4 and 5 exhibit similar results as with the 2023 contracts.

Expiration	$\beta = 0.25$	$\beta = 0.5$	$\beta = 0.75$	$\beta = 1$
March 2022	0	0	0	0
June 2022	0	0	0	0
September 2022	0	0	0	0
December 2022	0	0.01	0	0

Table 5: RMSE for the solutions of system (23). Numbers rounded to the sixth decimal place.

long maturity SOFR futures is quite low and even lower for options on these contracts. Second, as LIBOR publication is expected to cease by 2023, we are not comfortable about using contracts on LIBOR whose maturities are longer than this date.

5 Conclusion

We review the model introduced in Willems (2020) for reproducing smiles for backward and forward-looking caplets. We find that the effective parameters allow the model to incorporate both smiles under very limited conditions, which is due to their entire reliance on the parameter controlling the speed of decay of volatility. This limitation is confirmed after calibrating the model to market data.

In order to address this limitation, the effective parameters are modified in the same spirit as the original model of Hagan et al. (2018). The new effective parameters allow the model to incorporate both types of options with great accuracy.

A Pricing formulas

- The Black formula from Black (1976) is defined as:

$$Black(R, K, \sigma, T) = \left[RN\left(\frac{\ln(R/K) + (\sigma^2/2)\,T}{\sigma\sqrt{T}}\right) - KN\left(\frac{\ln(R/K) - (\sigma^2/2)\,T}{\sigma\sqrt{T}}\right)\right]$$

  where $N(*)$ denotes the CDF of the standard normal distribution.

- The IV approximation in Hagan et al. (2002) is given by:

$$\begin{aligned}
\sigma_{hagan}(R, K, \alpha, \beta, \rho, \nu, T) &= A \cdot \left(\frac{z}{\chi(z)}\right) \cdot B \\
A &= \frac{\alpha}{(RK)^{\frac{1-\beta}{2}}\left[1 + \frac{(1-\beta)^2}{24}\ln^2\frac{R}{K} + \frac{(1-\beta)^4}{1920}\ln^4\frac{R}{K} + \dots\right]} \\
B &= \left[1 + \left(\frac{(1-\beta)^2}{24}\frac{(\alpha)^2}{(RK)^{1-\beta}} + \frac{\rho\beta\nu\alpha}{4(RK)^{\frac{1-\beta}{2}}} + \frac{2-3\rho^2}{24}\nu^2\right) \cdot T + \dots\right] \\
z &= \frac{\nu}{\alpha}(RK)^{\frac{1-\beta}{2}} \ln\frac{R}{K} \\
\chi(z) &= \ln\left(\frac{\sqrt{1 - 2\rho z + z^2} + z - \rho}{1-\rho}\right)
\end{aligned}$$

The formulas for the effective parameters defined in Willems (2020) are:
When $0 < t < \tau_0$:

$$\hat{\rho} = \frac{2\rho}{\sqrt{\zeta}(3q+2)}, \quad \hat{\nu}^2 = \nu^2\zeta(2q+1), \quad \hat{\alpha}^2 = \frac{\alpha^2}{2q+1}\left(\frac{\tau_1}{\tau_1 - \tau_0}\right)^{2q} \mathrm{e}^{\frac{1}{2}\left(\frac{\nu^2}{q+1} - \hat{\nu}^2\right)\tau_1},$$

where:

$$\zeta = \frac{3}{4q+3}\left(\frac{1}{2q+1} + \rho^2\frac{2q}{(3q+2)^2}\right)$$

. When $\tau_0 < t < \tau_1$:

$$\hat{\rho} = \rho\frac{3\tau^2 + 2q\tau_0^2 + \tau_1^2}{\sqrt{\gamma}(6q+4)}, \quad \hat{\nu}^2 = \nu^2\gamma\frac{2q+1}{\tau^3\tau_1}, \quad \hat{\alpha}^2 = \frac{\alpha^2}{2q+1}\frac{\tau}{\tau_1}\mathrm{e}^{\frac{1}{2}H\tau_1}$$

where:

$$\tau = 2q\tau_0 + \tau_1, \quad H = \nu^2 \frac{\tau^2 + 2q\tau_0^2 + \tau_1^2}{2\tau_1 \tau (q+1)} - \hat{\nu}^2$$
$$\gamma = \tau \frac{2\tau^3 + \tau_1^3 + (4q^2 - 2q)\,\tau_0^3 + 6q\tau_0^2\tau_1}{(4q+3)(2q+1)} + 3q\rho^2\,(\tau_1 - \tau_0)^2\,\frac{3\tau^2 - \tau_1^2 + 5q\tau_0^2 + 4\tau_0\tau_1}{(4q+3)(3q+2)^2}$$

B Explicit formulas from lemma 3

- $\Delta_0^2 = \frac{{\alpha_0}^2\,\tau_0 - \frac{{\alpha_1}^2\,(\tau_0-\tau_1)}{2\,q+1}}{\tau_1}$
- $\bar{b}_0 = \frac{2\,\Delta_0^2\tau_1\,\left(\alpha_1\,\nu_0\,\rho_0\,\tau_0 - \frac{\alpha_1\,\nu_1\,\rho_1\,(\tau_0-\tau_1)}{q+1}\right) - {\alpha_0}^3\,\nu_0\,\rho_0\,{\tau_0}^2 + \frac{2\,\alpha_1\,\nu_1\,\rho_1\,(\tau_0-\tau_1)\,\left({\alpha_0}^2\,\tau_0(3q+2)+{\alpha_1}^2(\tau_1-\tau_0)\right)}{(3q+2)(q+1)}}{\Delta_0^4\tau_1^2}$
- $\bar{c}_0 =$

$$\frac{{\nu_0}^2\,\tau_0\,(2\,q+1)(\lambda - \alpha_1^2(\tau_0-\tau_1))}{\lambda^2} + \frac{3{\alpha_0}^4\,{\nu_0}^2\,{\rho_0}^2\,{\tau_0}^3}{\left(\Delta_0^2\tau_1\right)^3} - \frac{144\,{\alpha_1}^4\,{\nu_1}^2\,{\rho_1}^2\,(\tau_0-\tau_1)^3}{(4\,q+3)\left(\Delta_0^2\tau_1\right)^3}$$
$$- \frac{6\,{\alpha_1}^3\,\nu_1\,\rho_1\,(\tau_0-\tau_1)^2\,(\alpha_0\,\nu_0\,\rho_0\,\tau_0 + 3\,\alpha_1\,\nu_1\,\rho_1\,(\tau_1-\tau_0))}{(3q+2)\left(\Delta_0^2\tau_1\right)^3}$$
$$+ \frac{9{\alpha_1}^2\,(\tau_1-\tau_0)\,(\alpha_0\,\nu_0\,\rho_0\,\tau_0 + 2\,\alpha_1\,\nu_1\,\rho_1(\tau_1-\tau_0))^2}{(2\,q+1)\left(\Delta_0^2\tau_1\right)^3}$$
$$+ \frac{{\alpha_1}^4\,(2\,q+1)\,(\tau_0-\tau_1)^2\,({\nu_0}^2\,\tau_0(3+4q) + 3\,{\nu_1}^2(\tau_1-\tau_0))}{(4\,q+3)\,\lambda^3} - 3\bar{b}_0^2$$

where:
$\lambda = {\alpha_0}^2\,(\tau_0 + 2\,q\,\tau_0) + {\alpha_1}^2(\,\tau_1 - \tau_0)$

- $G_0 = -\frac{{\alpha_1}^2\left(\frac{{\nu_1}^2\,(\tau_0-\tau_1)^2}{q+1} + \frac{2\,(\tau_0-\tau_1)\,\left({\nu_0}^2\,\tau_0 - {\nu_1}^2\,(\tau_0-\tau_1)\right)}{2\,q+1}\right) - {\alpha_0}^2\,{\nu_0}^2\,{\tau_0}^2}{\left(\Delta_0^2\tau_1\right)^2} - \bar{c}_0$
- $\Delta_1^2 = \frac{\alpha_1^2}{2q+1}\left(\frac{\tau_1}{\tau_1-\tau_0}\right)^{2q}$
- $\bar{b}_1 = \frac{\nu_1\rho_1(4q+2)}{\alpha_1(3q+2)}\left(\frac{\tau_1-\tau_0}{\tau_1}\right)^{q}$
- $\bar{c}_1 = \frac{3\,\nu_1^2\,\left((\tau_0-\tau_1)^2\right)^q\,(2\,q+1)\,\left(3\,q+12\,q\,\rho_1^2+6\,\rho_1^2+2\right)}{\alpha_1^2\,{\tau_1}^{2\,q}\,(3\,q+2)\,(4\,q+3)} - 3\bar{b}_1^2$
- $G_1 = \frac{\nu_1^2}{\Delta_1^2(q+1)} - \bar{c}_1$

References

Bailey, Andrew. 2017. *The future of LIBOR,* July. https://www.fca.org.uk/news/speeches/the-future-of-libor#webform-submission-page-feedback-form-node-44376-add-form.

Black, Fischer. 1976. "The pricing of commodity contracts." *Journal of financial economics* 3 (1-2): 167–179.

Chen, Bin, Lech A Grzelak, and Cornelis W Oosterlee. 2011. "Calibration and Monte Carlo pricing of the SABR-Hull-White model for long-maturity equity derivatives." *The Journal of Computational Finance (79–113) Volume* 15.

CME. 2020. *Exploring options on one-month SOFR Futures,* December. https://www.cmegroup.com/education/articles-and-reports/options-on-one-month-sofr-futures.html.

Crispoldi, Christian, Gérald Wigger, and Peter Larkin. 2016. *SABR and SABR LIBOR Market Models in Practice: With Examples Implemented in Python.* Springer.

Feldman, Konstantin. 2021. "Analytic Calibration in Andreasen-Huge SABR Model." *Wilmott* 2021 (114): 62–69.

Floc'h, Le, Gary J Kennedy, et al. 2014. "Explicit SABR Calibration Through Simple Expansions." *Available at SSRN 2467231.*

Gauthier, Pierre, and Pierre-Yves Henri Rivaille. 2009. "Fitting the smile, smart parameters for SABR and Heston." *Smart Parameters for SABR and Heston (October 30, 2009).*

Hagan, Patrick S, Deep Kumar, Andrew S Lesniewski, and Diana E Woodward. 2002. "Managing smile risk." *The Best of Wilmott* 1:249–296.

Hagan, Patrick S, Andrew S Lesniewski, and Diana E Woodward. 2018. "Managing vol surfaces." *Wilmott* 2018 (93): 24–43.

Henrard, Marc Pierre. 2019. "LIBOR fallback and quantitative finance." *Risks* 7 (3): 88.

Lyashenko, Andrei, and Fabio Mercurio. 2019. "Looking forward to backward-looking rates: A modeling framework for term rates replacing LIBOR." *Available at SSRN 3330240.*

Piterbarg, Vladimir. 2020. "Interest rates benchmark reform and options markets." *Available at SSRN 3537925.*

Rebonato, Riccardo, Kenneth McKay, and Richard White. 2009. *The SABR/LIBOR Market Model: Pricing, calibration and hedging for complex interest-rate derivatives.* John Wiley & Sons.

Skov, Jacob Bjerre, and David Skovmand. 2021. "Dynamic Term Structure Models for SOFR Futures." *arXiv preprint arXiv:2103.11180.*

Van der Stoep, Anthonie W, Lech A Grzelak, and Cornelis W Oosterlee. 2015. "The time-dependent FX-SABR model: Efficient calibration based on effective parameters." *International Journal of Theoretical and Applied Finance* 18 (06): 1550042.

Wang, Zaizhi. 2007. "'Effective'Parameters for Stochastic Volatility Models." In *Paris December 2007 Finance International Meeting AFFI-EUROFIDAI Paper.*

West, Graeme. 2005. "Calibration of the SABR model in illiquid markets." *Applied Mathematical Finance* 12 (4): 371–385.

West, Graeme. 2009. "South African financial markets." *Financial Modelling Agency (September 2009).*

Willems, Sander. 2020. "SABR smiles for RFR caplets." *Available at SSRN 3567655.*

Wu, Qi. 2012. "Series expansion of the SABR joint density." *Mathematical Finance: An International Journal of Mathematics, Statistics and Financial Economics* 22 (2): 310–345.

Zhang, Mengfei, and Frank J Fabozzi. 2016. "On the Estimation of the SABR Model's Beta Parameter: The Role of Hedging in Determining the Beta Parameter." *The Journal of Derivatives* 24 (1): 48–57.